NATIONAL RADIO ASTRONOMY OBSERVATORY
SOCORRO, NEW MEXICO
VERY LARGE ARRAY

VLA SCIENTIFIC MEMORANDUM 149

DECONVOLUTION WITH A MAXIMUM ENTROPY TYPE ALGORITHM

Tim Cornwell

July 1983

Abstract : A simple, efficient MEM type deconvolution algorithm now implemented in AIPS (VM) is described. It allows use of any of a number of uniformity functions with optional specifiable upper and lower brightness limits. Control parameters are the r.m.s. residual expected (Jy/beam) and the total flux in the image. With correct values it seems that high quality images can be obtained. The question of reliability of super-resolution is discussed. A full discussion of the properties of VM images is presented.

The Problem :

CLEAN (Hogbom 1974, Schwarz 1978) sometimes fails to produce aesthetically pleasing deconvolutions of VLA images. Trusting our knowledge of the structures of radio sources we might go further and suggest that it sometimes produces an incorrect answer. Thus CLEAN must be implicitly assuming the wrong sort of information about typical radio sources. Let us remind ourselves of the assumptions built into CLEAN : first, the sky should be mainly empty so that only a small region of the primary beam is to be estimated, secondly, any emission can be modelled by a set of delta functions. This second assumption can lead to two problems when imaging regions of extended emission : slow convergence and instabilities such as mottling or striping. To avoid these drawbacks we should replace the assumption of "pointed-ness" by some other reasonable characteristic of radio sources. In this paper we will choose uniformity, roughly defined as the tendency of pixel brightness to cluster in a histogram. We will also extend the first assumption to include knowledge of any uniform background on which the radio source sits. Our optimum algorithm will thus choose the image which :

1. Is as uniform as possible AND
2. Lies within some well defined brightness limits.

The presence of noise in the visibility data will nearly always prevent such an image from fitting the data exactly so we will require that :

3. the r.m.s. residual should be that expected.

It is difficult to see how CLEAN can be modified to obey these constraints so we will have to develop an optimisation routine so that the

final image simultaneously obeys these constraints. The third constraint requires calculation and optimisation of the residuals, aiming at some target value, and obedience to the second constraint can be enforced with simple constrained optimisation techniques. The uniformity constraint (1) requires some measure of clustering of pixel values; some of the many functions which can be used for this purpose are :

$$S_0 = \Sigma_i \, -b_i^{\,2}$$

$$H_1 = \Sigma_i \, -b_i . \ln(b_i)$$

$$H_2 = \Sigma_i \, \ln(b_i)$$

$$S_3 = \Sigma_i \, (b_i)^{1/2}$$

$$S_4 = \Sigma_i \, -(b_i)^{-1}$$

H_1 and H_2 are the well known entropy functions which may or may not have some deep philosophical underpinning; we will ignore this possibility to concentrate merely upon the uniformity preference (see e.g. Wernecke 1977). If the total power is fixed then all these measures are maximised for completely smooth images in which the emission is spread smoothly over the field of view. All, except for S_0, act as a barrier function in any optimisation; that is, if the initial estimate is totally positive then any reasonable gradient-sensitive optimisation procedure will keep subsequent images totally positive. This is clearly desirable when dealing with known limits on the brightness. We can generalise these forms to include upper and lower bounds e.g. :

$$H_2 = \Sigma_i \, (\ln(b_i - b_{lower}) + \ln(b_{upper} - b_i))$$

All pixel brightnesses will be kept in the range b_{lower} to b_{upper}. Such a function is of use in deconvolving images of planets (e.g. Nityananda and Narayan 1982). Other extensions, such as position dependent brightness limits, may be advantageous in some circumstances at little extra computational cost.

Thus our optimum algorithm is simply a variant of the Maximum Entropy method except that in the latter either H_1 or H_2 is used (Wernecke and D'Addario 1976, Gull and Daniell 1978). However, we place no undue emphasis upon the form of the uniformity measure. To distinguish our algorithm from MEM we will, in common with Nityananda and Narayan (1982), call it the variational method VM.

Formulation of the solution :

The residuals for interferometry are independent in the u,v plane and so the residuals are of the form :

$$\chi^2 = \Sigma_i \, w_i \, |T_i - B_i|^2$$

where w_i is the weight assigned to the i'th visibility sample, T_i is the i'th visibility sample and B_i is the Fourier transform of the image $\underline{b}$ at the corresponding u,v point. This can also be written in the image plane (see e.g. Wernecke and D'Addario 1976), using an obvious vector notation :

$$\chi^2 = (\underline{t} - \underline{b})^T . p . (\underline{t} - \underline{b})$$

where p is the beam and $\underline{t}$ is any solution to the convolution equation:

$$p . \underline{t} = \underline{d}$$

where $\underline{d}$ is the dirty image. We select the units of $\underline{b}$ to be Jy pixel^{-1}. The algorithm must solve the problem :

$$\text{Maximise } H(\underline{b}) \text{ subject to } \chi^2 = 2.N_{vis}.\sigma^2$$

where σ is the r.m.s. noise in the real or imaginary part of the visibility, and N_{vis} is the number of visibility samples. If the total flux is not constrained then, in the absence of an upper limit in brightness, the VM image will have a very large bias in the total flux and, in compensation, will over-fit to the other spatial frequencies. This is just the principal solution raised upon a large pedestal (Bhandari 1978). For this reason it is important to specify and fit to the total flux accurately and so we add an extra condition, namely that:

$$F = F_{obs} \text{ where } F = \Sigma_i \, b_i$$

and F_{obs} is the observed total flux. This is equivalent to accurate knowledge of the baseline. Furthermore, this constraint is much stronger if there are large areas of no emission and so, like CLEAN, VM works best when most of the sky is empty.

Equivalently, we maximise the uniformity subject to the constraint that the first two moments of the distribution of the residuals equal the expected values. The Lagrange multiplier approach is useful for this problem. We reformulate the problem :

$$\text{Maximise } J(\underline{b}) = H(\underline{b}) - \alpha.\chi^2/2 - \beta.F$$

where α and β are chosen so that :

1. $F - F_{obs} = \Sigma_i \, b_i - F_{obs} = 0.0$ - first moment of residuals
2. $\chi^2 = 2.N_{vis}.\sigma^2$ - second moment of residuals

Since χ^2 is awkward to calculate and, having units $Jy^2\ beam^{-1}\ pixel^{-1}$, is not related to any simple observable we will replace constraint 2 by:

$$2.'\ E = E_{obs} = N_{pixel} \cdot \sigma_{image}^{\ 2}$$

where $$E = (\underline{t} - \underline{b})^T . p^T . p . (\underline{t} - \underline{b})$$

and σ_{image} is the expected r.m.s. noise in the dirty image, and N_{pixel} is the number of pixels in the image. This latter quantity, which has units Jy $beam^{-1}$, can be either calculated a priori or measured from a CLEAN image. Note that E is only used as a target in the optimisation and that J still contains χ^2 since the statistics of the residuals demand it. If the noise were independent in the image plane, as it is in the optical case, then we would use E in J directly.

An algorithm to maximise J :

One obvious approach is to use an ordinary first order gradient search method. For each iteration one would perform a search in the direction $\underline{\nabla J}$:

Choose γ to maximise $J(\underline{b}')$ where the new estimate is $\underline{b}' = \underline{b} + \gamma . \underline{\Delta b}$ and

$$\underline{\Delta b} = \underline{\nabla J} = \underline{\nabla H} - \alpha . \underline{\nabla \chi^2}/2 - \beta . \underline{1}$$

Such optimisation of J is difficult because of the extremely non-linear behaviour of H near the brightness limits, e.g. zero, where most of the true pixel values reside. Small changes in weak pixels can alter H drastically while having little effect on the residuals. This means that the normal first order gradient search method is extremely wasteful since for pixels which are near the boundaries $\underline{\nabla J}$ does not point towards the true minimum. A second order correction is required to redirect the vector; this leads to the Newton-Raphson approach :

$$\underline{\Delta b} = (-\nabla\nabla J)^{-1} . \underline{\nabla J}$$

The new factor is the Hessian matrix :

$$\nabla\nabla J = \nabla\nabla H - \alpha . p$$

which has dimension N_{pixel}^2 and obviously cannot be inverted. However, the most important part is $\nabla\nabla H$ which is diagonal (see Cornwell 1980). Hence, neglecting the sidelobes of the beam, we obtain :

$$((-\nabla\nabla J)^{-1})_{i,i} \simeq (- (\nabla\nabla H)_{i,i} + \alpha . p_{i,i})^{-1}$$

$$((-\nabla\nabla J)^{-1})_{i,j} \simeq 0.0 \qquad i \neq j$$

With this approximation the Newton-Raphson approach is practicable. A quadratic search in the direction $\underline{\Delta b}$ requires evaluation of $\underline{\nabla J}$ at two places, requiring two convolutions or four FFTs. The convolution sum for the optimum point along the search direction can be interpolated at relatively little extra cost. Thus the average cost per iteration is two FFTs plus a number of file reads. We use this metric to measure distances, e.g. :

$$|| \underline{\nabla X} ||^2 = \underline{\nabla X}^T . (-\nabla\nabla J)^{-1} . \underline{\nabla X}$$

Some control procedures are needed. A good choice for the initial image is :

$$b_i = F_{obs}/N_{pixel} \text{ for all pixels.}$$

The maximum step length should be limited to some reasonable value (see e.g. Skilling and Gull 1983). We limit :

$$\underline{\nabla J}^T . \underline{\Delta b} < g . \alpha . E_{current}$$

where g is a gain factor, typically 0.5. Sensible initial values of α and β are required. On dimensional grounds we use :

$$\alpha_{initial}^2 = 4.0.|| \underline{\nabla}H||^2/|| \underline{\nabla}\chi^2||^2$$

$$\beta_{initial}^2 = || \underline{\nabla}H||^2/|| \underline{\nabla}F||^2$$

These values are always underestimates of the correct values so it is also necessary to iterate α and β to force the VM image to obey the constraints. For efficiency, changes in these values should be allowed only when a valid solution has been obtained with the current values. A suitable criterion for a solution involves the expected change in J : $\underline{\nabla}J^T.\ \underline{\Delta b}$, if this is less than $\alpha.E$ we alter α and β by the increments :

$$\Delta\alpha/\alpha = (E_{current}/E_{obs}) - 1$$

$$\Delta\beta/\beta = (F_{current}/F_{obs}) - 1$$

allowing a maximum fractional change of g. These steps may be regarded as performing a search in E,F,α,β space.

Since sometimes a negative pixel may be chosen, we protect against this by clipping moves at the levels:

$$(1-g).b_{max} + g.b_{upper} > b_i > (1-g).b_{min} + g.b_{lower}$$

where b_{upper} is the specified upper bound and b_{max} is the previous maximum in the image; similarly for the lower bound.

Finally, the stopping criterion is :

a. $\underline{\nabla}J^T.\ \underline{\Delta b} < 0.5.\alpha.E_{obs}$ AND

b. $|E_{obs} - E_{current}| < 0.05.E_{obs}$ AND

c. $|F_{obs} - F_{current}| < 0.05.F_{obs}$

These latter two tolerances reflect upper bounds in accuracy of E_{obs} and F_{obs}.

Wernecke and D'Addario (1976) produced the first MEM algorithm used in radio-astronomy but they neglected to enforce the first moment constraint, and they failed to iterate to the true value of α. For these two reasons their algorithm did not achieve the full power of the VM.

Our algorithm is similar to that of Skilling and Gull (1983) except that, in their algorithm :

1. Optimum values of α and β are found at each iteration by searching in three independent directions and thus 6 FFTs per iteration are required. The success of our simpler algorithm indicates that such sophistication may not be necessary if sensible schemes for choosing and updating α and β are used.
2. H_1 is always used and the pixel brightness is normalised by F_{obs}. We see no fundamental reason to favour any

uniformity form and have chosen to use S_3 for convenience and to avoid any dubious interpretation of the meaning of a VM image.

3. $\nabla\nabla H$ is used as an approximation to $\nabla\nabla J$; we find that this slows convergence unacceptably.

The paper of Skilling and Gull (1983) gives some useful tips on the design of a VM algorithm and, in particular, on the importance of the metric.

Nityananda and Narayan (1982) propose that since the form of the VM image is critically dependent upon the total flux, this quantity should be adjusted to yield an image of preferred properties, such as resolution. We find this argument to be at variance with the philosophy expressed here, namely that one should apply as many valid constraints as possible. In many cases the total flux is known to a reasonable accuracy and can be used to impose useful bounds upon the possible VM image. If the total flux is unknown then it seems to us unsound to estimate it from nebulous preferred image properties.

McClellan and Lang (1983) have argued that the dual optimisation approach, effectively operating in the u,v plane, is preferable since it is intrinsically finite-dimensional unlike the primal algorithm considered here which is merely a discrete approach to an infinite-dimensional problem. However, in their algorithm it is still necessary to evaluate Fourier transforms on a very fine grid so little practical advantage arises from the dual algorithm. Also they neglect to enforce the first moment constraint on the residuals and for that reason will obtain unduly noisy VM images.

Some Properties of VM images

Some properties of VM images can be deduced from the defining equations.

1. Resistance to noise : To first order we may neglect the dependence of of the estimate on α and so the sensitivity to noise is given by the inverse Hessian :

$$(-\nabla\nabla J)^{-1} = (-\nabla\nabla J + \alpha.p)^{-1}$$

Since the beam p has sidelobes which extend over all the image all points in the VM image are correlated. Thus for a true noise analysis the Hessian must be inverted, which is, for most images, totally impractical. Under certain assumptions, such as banded-ness of p, equivalent to a limitation in the extent of the beam sidelobes, an approximation to the inverse may be satisfactory. This is an interesting topic for further work.

We can investigate the basic character of the noise behaviour by neglecting the sidelobes of the beam (Cornwell 1980). The inverse then only has diagonal elements:

$$((-\nabla\nabla J)^{-1})_{i,i} \simeq (-(\nabla\nabla H)_{i,i} + \alpha.p_{i,i})^{-1}$$

For the example of H_2 we have, if $b_{upper} \rightarrow \infty$ and $b_{lower} = 0$:

$$\sigma_{b_i}^2 = ((-\nabla\nabla J)^{-1})_{i,i} \simeq (b_i^{-2} + \alpha.p_{i,i})^{-1}$$

For weak points the relative error is constant whereas for strong points the absolute error is constant. Note that, as mentioned above, adding a large offset to each pixel will produce an image in which the absolute error is constant all over the image. Therefore the value of the total power F is very important as a constraint.

In table I we show the asymptotic errors for a variety of uniformity measures for general brightness limits.

TABLE I. Asymptotic errors.

uniformity form	σ_b	
	Near limits	Far from limits
H_1	$\alpha\ \delta b^{1/2}$	$\alpha\ \sigma_{image}$
H_2	$\alpha\ \delta b$	$\alpha\ \sigma_{image}$
S_3	$\alpha\ \delta b^{3/4}$	$\alpha\ \sigma_{image}$
S_4	$\alpha\ \delta b^{3/2}$	$\alpha\ \sigma_{image}$

The distance of a pixel from a brightness limit is δb.

Finally, we note that this is only an analysis of the stability of the VM image to noise, not an analysis of its stability to changing u,v plane coverage.

2. Sensitivity to u,v plane coverage : The VM image must change as the u,v plane coverage changes or, equivalently, as the sidelobe structure of the beam changes. This effect is calculable to first order but again involves the inversion of $\nabla\nabla J$, which is, in all practical cases, not possible.

If such information is required it may be simpler to perturb p slightly and continue the iteration to the new VM image.

3. The residuals of an VM image are not random : The residual image is :

$$p.(\underline{b} - \underline{t}) = \underline{\nabla\chi}^2/2$$

Hence, from the condition that the gradient of J be zero at the VM image we have that :

$$p.(\underline{b} - \underline{t}) = (\underline{\nabla H} - \beta. \underline{1})/\alpha$$

Thus, the VM image is almost certainly incorrect since the probability of such a set of residuals is vanishingly small (see also Bryan and Skilling 1980).

4.

The size ascribed to an isolated point source in an VM image varies with signal to noise : This SNR-dependent resolution arises because VM images are always biased towards greater uniformity or smoother images and as the SNR decreases the leeway for smoothing increases. It is instructive to consider this effect in the u,v plane. Longer spacings are systematically underestimated as much as allowed by the constrained value of E; increased noise allows greater underestimation. A number of fixes for this problem are possible :

a. Use a minimax criterion for the data fitting : chose the image which has maximum uniformity and for which the maximum residual is minimised. Minimax methods are much more time-consuming than least squares methods, probably prohibitively so for problems of the large dimensionality encountered in image construction.

b. Fit to the data as well as possible. The noise then propagates to higher spatial frequencies and the apparent image quality decreases. For most data sets a perfect fit is impossible.

c. Minimise a linear sum of χ^2 for different regions on the u,v plane, constraining a fit to the expected value within each region. Again, practical implementation will be difficult.

d. Require that the distribution of residuals be Normal (see e.g. Bryan and Skilling 1980). This only alleviates the problem since underestimation at long spacings still occurs.

e. Constrain more moments of the residual distribution than just the first two moments.

f. Constrain the information-theoretic entropy of the residuals to be equal to the expected value. In the current algorithm entropy has been removed from the residuals and structure has been removed from the VM image. It may be possible to approximately measure $H_{residuals}$ and optimise with that constraint replacing the constraints on F and χ^2.

All these options lead to increased computing requirements and, for that reason, are probably not worth a great deal of effort. We should note that if one of these schemes were implemented then the super-resolution in the VM image would increase slightly leading to further doubts about reliability.

Much has been made of the SNR dependence of the resolution since it would seem that this should prevent the use of VM images in spectral index calculations. However, if one first convolves the VM images with the analogue of a CLEAN beam then it should be possible to make such comparisons between different images. The sufficient condition is that for all regions of interest the effective resolution should be much less than that of the CLEAN beam. We postulate that this will always be true if there is enough signal to allow calculation of the spectral index from a pair of CLEAN images. In support of this view we note that one would be extremely foolish to make spectral index images from unconvolved CLEAN images. Some results concerning this point are given below.

5. Gibbs oscillations : VM images are especially subject to Gibbs oscillations near sharp edges since the data can be best fit by allowing such oscillations. This can be alleviated to some degree by imposing upper bounds on the brightness just as lower bounds are imposed. Some examples of Gibbs oscillations are shown below.

6. Sensitivity to uniformity form : Gull and Daniell (1978) have asserted that, if only the second moment constraint on the residuals is enforced, maximising H_1 with the pixel brightness normalised by the total flux yields superior results than maximising any other form, but in particular H_2, with no normalisation. Since the normalisation requires that the total flux be fit this is in complete accord with our observation that the first moment constraint on the residuals must be enforced to protect against noise.

7. Sensitivity to control parameters : After convergence, the VM image is determined by a number of controlling parameters :

a. Specified residual σ_{image}. Higher values produce smoother images. Low values may prevent a fit and will produce a spikier image.

b. Specified total flux F_{obs}. High values allow bigger sidelobes. Low values may prevent a fit.

c. Bounds in brightness b_{upper}, b_{lower}. Accurate limits force flat baselines and plateaus. Inaccurate values may allow ripples or may prevent a fit.

Other parameters such as the gain g, or the path taken to the estimate should not affect the final image. Thus, for example, one may keep refining the dirty image by selfcalibration (Schwab 1980) or data editing while iterating using the same VM image. One can iterate for a while, then selfcalibrate or edit, then continue VM iteration with a new dirty image and the old VM image.

Some Examples :

The first set of tests illustrate the effect of changing the uniformity measure. Artifical data corresponding to a Gaussian of FWHM about 5 beam-widths and peak S/N of about 100 in the dirty image were used. Figure 1 shows the discrepancies of the VM images, a CLEAN image and a smoothness stabilised CLEAN image from the original model. It is clear that there are no significant differences between the images produced from the different uniformity measures.

The second set of tests show the effect of overestimating the noise. In Figure 2 are shown the discrepancy from the model of H_1 VM reconstructions targeting on 2 and 3 times the true σ_{image}. As expected the images get smoother as the fit worsens. Note the very flat background in the VM images. The 3-σ image is noticeably biased with a large offset in the background. The VM images converged in about 20 iterations, which for these small images (128*128) took about 20 minutes wall clock time or about 7 minutes CPU time on a VAX 11/780 with FPS AP120B array processor.

Gibb oscillations can be a severe problem in VM images unless an upper limit in brightness is known and enforced. In figure 3 I show slices through VM reconstructions of a box, enforcing various levels of upper limit. The first image had no upper bound and consequently large oscillations occured at the edges of the box. Decreasing the upper bound shrinks down these oscillations, indicating that tighter constraints give better reconstructions.

Some reliable super-resolution from VLA data is possible. Figure 4 shows CLEAN and VM images of 3C449 made from C-array data and a CLEAN image made from B-array data. The latter two images agree to reasonable level especially so since some bad data is still present. That such super-resolution is possible is not too suprising since the u,v coverage for the VLA is quite often redundant and so some of the derivatives of the visibility function are known thus enabling, effectively, an analytic continuation. Another, contrary example is shown in Figure 5, where the B-array VM H_1 image and an A-array CLEAN map of 3C219 are plotted, the former after convolution with the clean beam of the latter. The size of these images is 1024*512 and the VM took about 2 hours of CPU time for convergence. However, the CLEAN took a comparable amount of time since only ~ 50 components were removed per major cycle. On the I^2S it is clear that VM has failed to remove the sidelobes of the dirty beam; it appears that the u,v coverage in this case is insufficent to allow the visibility function to be extrapolated. This example shows that, as with CLEAN, experience with VM is required for the reliability of images to be predictable.

Figure 6 shows various parts of CLEAN and VM images of Cygnus A at λ6cm made from the same A-array data. The levels plotted are as a percentage of a well resolved peak and therefore are equivalent in surface brightness. The peak signal to noise is 3000; convergence was acheived in 26 iterations or about 5 hours VAX CPU time. The resolution has improved markedly and is now limited by the pixel size; sizes of barely resolved components agree with those calculated from IMFIT (i.e. by beam deconvolution). The well resolved regions have the same overall structure but gradients are stronger in the VM image. No gross new features are seen on the VM image.

Some Conclusions :

VM will be useful in VLA data reduction for the analysis of images of large extended objects for which CLEAN is notoriously slow and inefficient. It is harder to control than CLEAN but sometimes gives better results. Super-resolution of compact, oversampled objects may also be possible, at least for qualitative results. In terms of FFTs required the current algorithm is roughly comparable to that of Skilling and Gull (1983) but it has some added flexibility in that brightness limits can be imposed and that the uniformity function can be selected. However, the effect of changing the uniformity function is minimal compared to the effect of specifying correctly the noise level and the zero spacing flux. We note that VM can be used to obtain the MEM solution for either H_1 or H_2.

The VM program described here is available in AIPS. We note that VM has an option to analyse optical data in which the noise is normally distributed and is independent from pixel to pixel.

Acknowledgements :

I thank Ron Ekers, Steve Gull and Don Wells for some useful discussions. Magdy T. Hanna provided some assistance in the programming of VM. I thank Rick Perley for the use of his 3C219 and Cygnus A data.

References :

Bhandari,R.,"Maximum Entropy spectral analysis - some comments", Astron. Astrophys. 70,331,1978.

Bryan,R.K., and Skilling,J., "Deconvolution by maximum entropy, as illustrated by application to the jet of M87",M.N.R.A.S., 191, 69-79,1980.

Cornwell,T.J., "The mapping of radio sources from interferometer data", Ph.D. Thesis, University of Manchester, 1980.

Gull,S.F. and Daniell,G.J.,"Image reconstruction from incomplete and noisy data",Nature, 272,686-690,1978.

Hogbom,J., "Aperture synthesis with a non-regular distribution of interferometer baselines",Astron. Astrophys. Suppl., 15,417,1974.

McClellan,J.H. and Lang,S.W., "Duality for multidimensional MEM spectral analysis",IEE Proc., 130, 230-235, 1983.

Nityananda, R., and Narayan, R., "Maximum Entropy image reconstruction - principles, practice and problems", J. Astrophys. Astr., 3, 419, 1982.

Schwab,F.R., "Adaptive calibration of radio interferometer data",SPIE, 231,18-24, 1980.

Schwarz,U.J., "Mathematical-statistical description of the iterative beam removing technique (method CLEAN)",Astronomy and Astrophysics, 65,345-356, 1978.

Skilling,J. and Gull,S.F., "Algorithms and applications", preprint, 1983.

Wernecke,S.J. and D'Addario,L.R., "Maximum entropy image reconstruction", IEEE C-26,351-364, 1976.

Wernecke,S.J., "Two dimensional maximum entropy reconstruction of radio brightness",Radio Science, 12,831-844,1977.

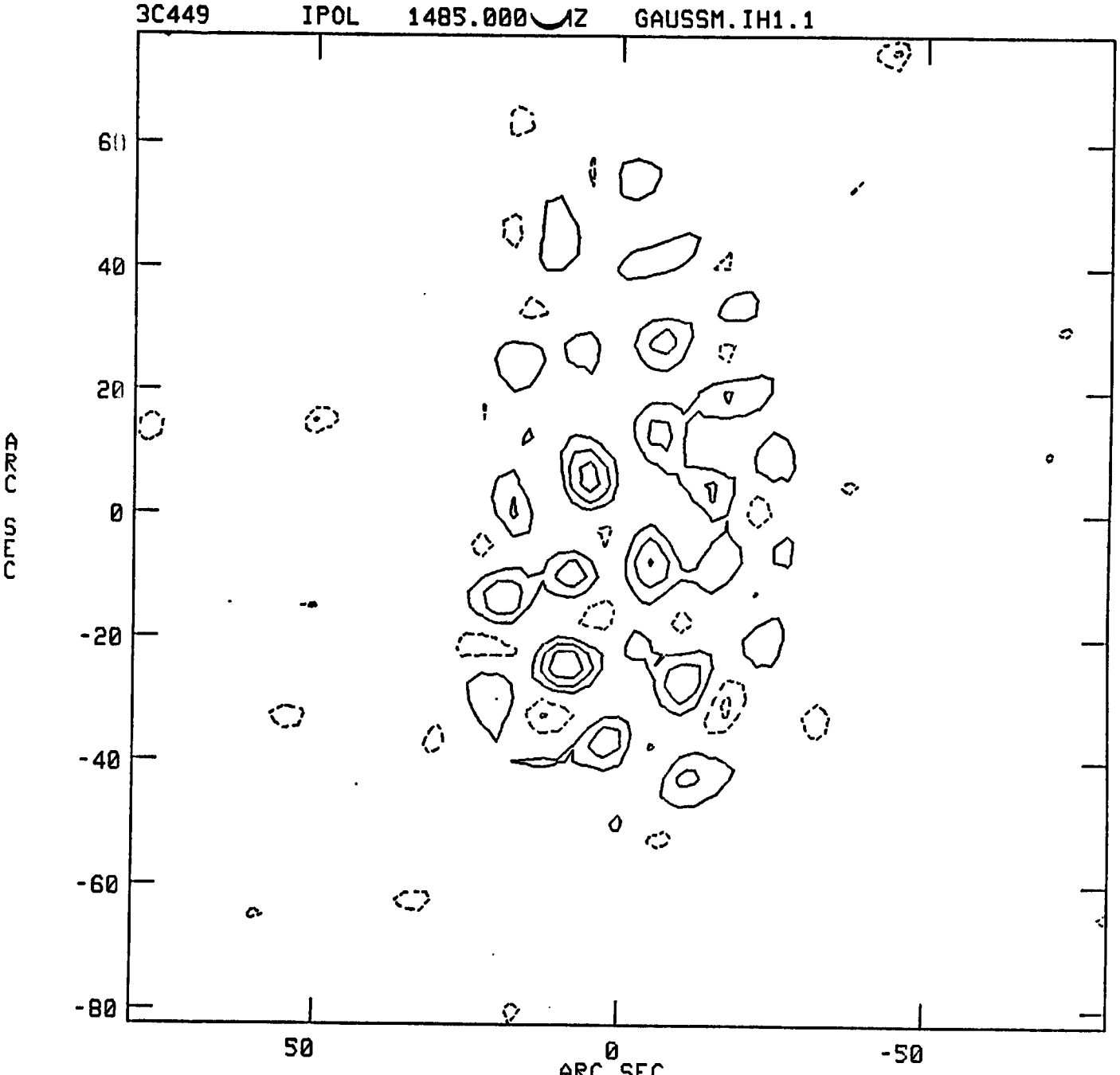

CENTER AT RA 22 29 07.629 DEC 39 06 03.50
PEAK FLUX = 1.9806E-04
LEVS = 0.5000E-04 * (-10.0, -9.0, -8.0,
-7.0, -6.0, -5.0, -4.0, -3.0, -2.0,
-1.0, 1.0, 2.0, 3.0, 4.0, 5.0,
6.0, 7.0, 8.0, 9.0, 10.0)

Fig 1

H_1 emag

True peak

$\sim 2\ 10^{-3}$

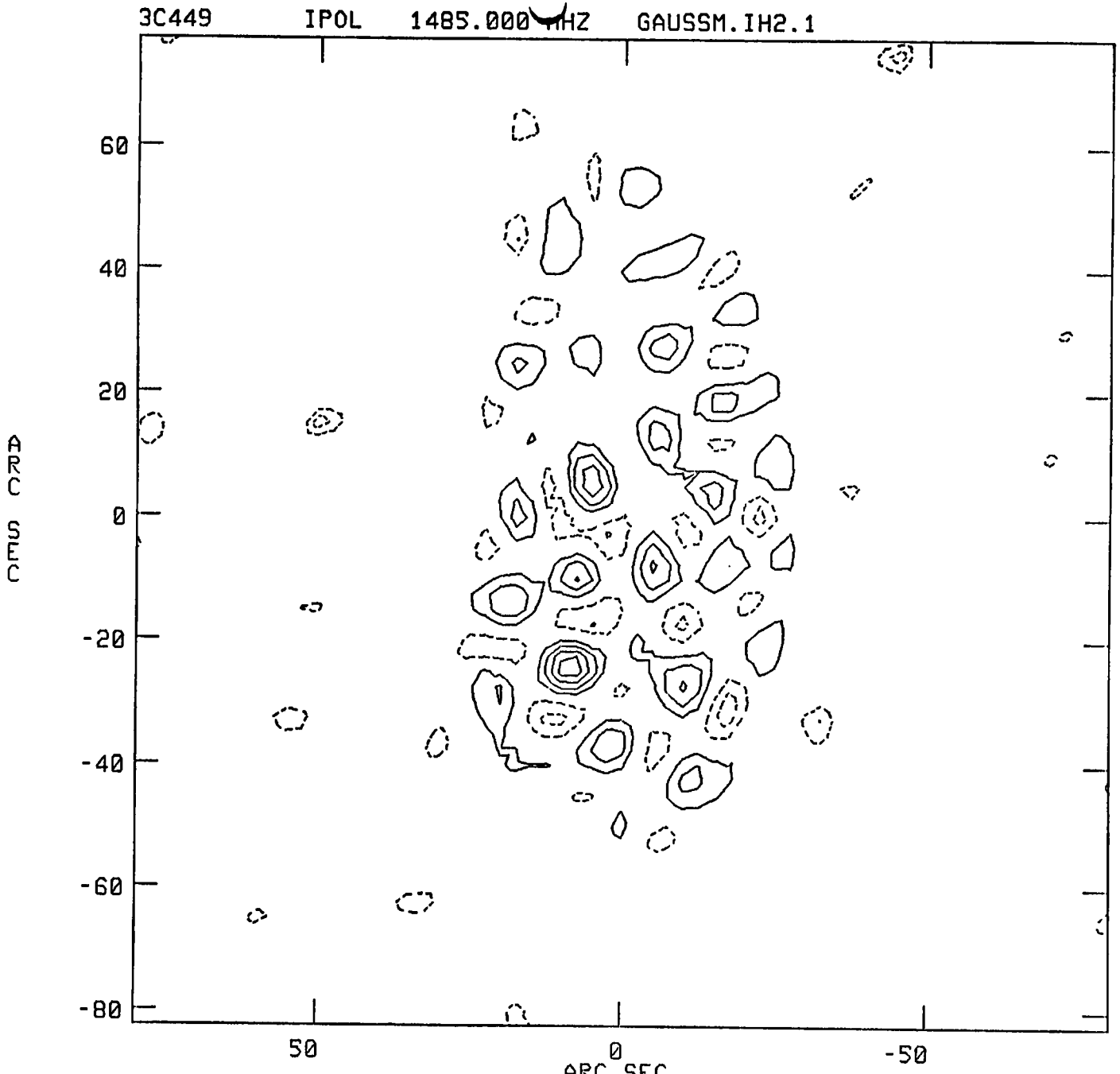

H_2 errors

CENTER AT RA 22 29 07.629 DEC 39 06 03.50
PEAK FLUX = 2.2746E-04
LEVS = 0.5000E-04 * (-10.0, -9.0, -8.0,
-7.0, -6.0, -5.0, -4.0, -3.0, -2.0,
-1.0, 1.0, 2.0, 3.0, 4.0, 5.0,
6.0, 7.0, 8.0, 9.0, 10.0)

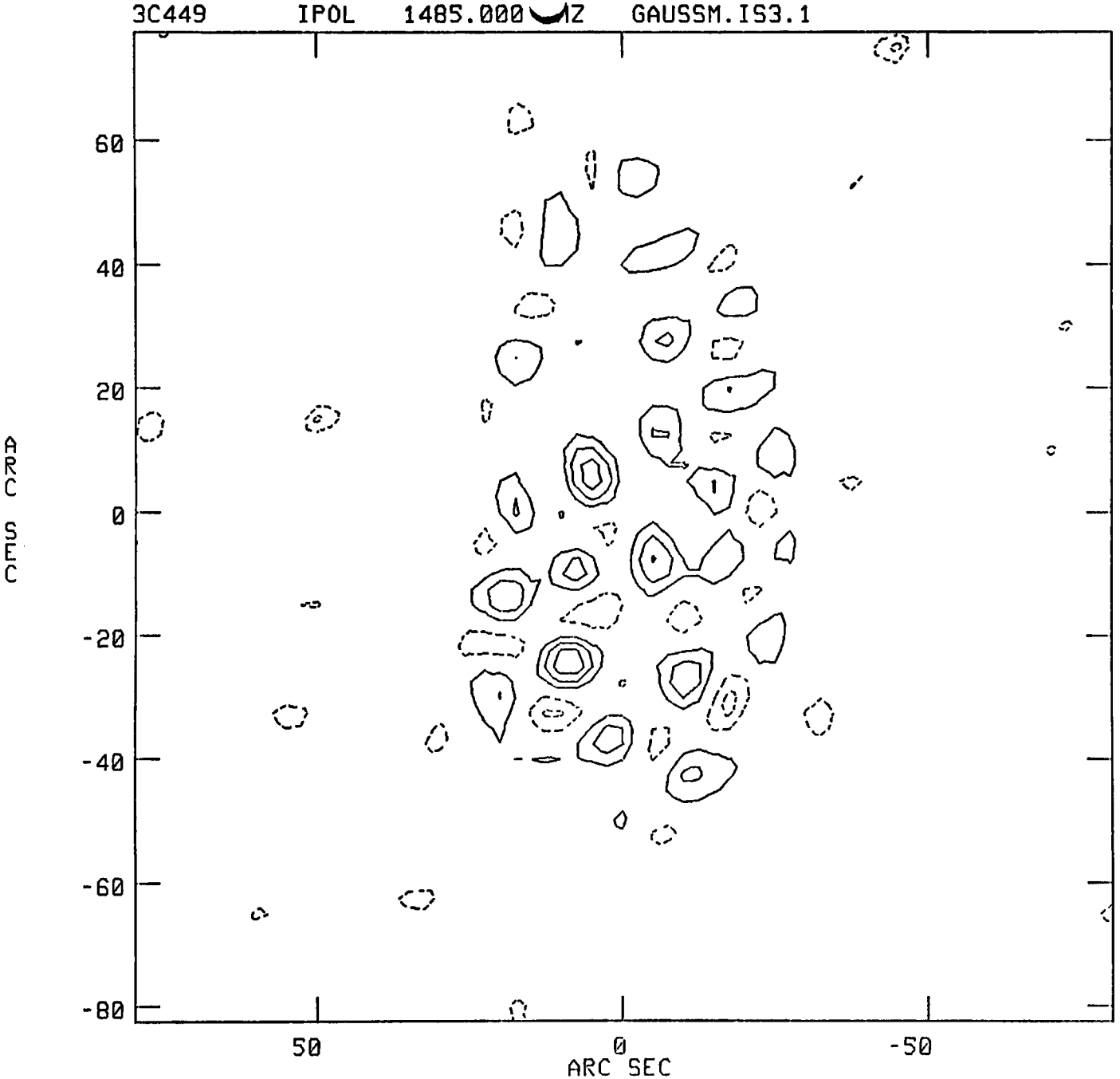

S_3 errors

CENTER AT RA 22 29 07.629 DEC 39 06 03.50
PEAK FLUX = 1.9177E-04
LEVS = 0.5000E-04 * (-10.0, -9.0, -8.0,
-7.0, -6.0, -5.0, -4.0, -3.0, -2.0,
-1.0, 1.0, 2.0, 3.0, 4.0, 5.0,
6.0, 7.0, 8.0, 9.0, 10.0)

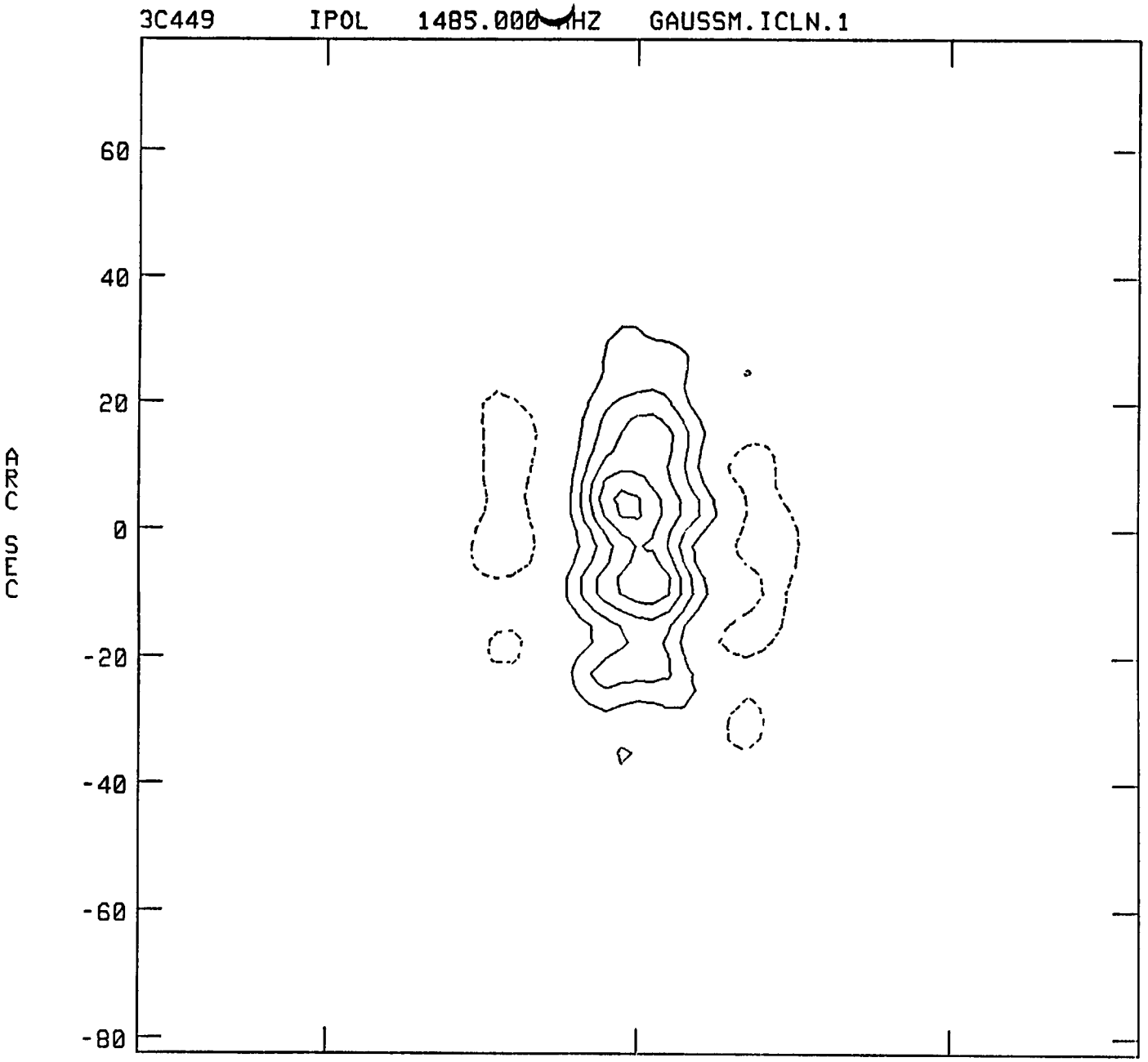

Clean enos

CENTER AT RA 22 29 07.629 DEC 39 06 03.50
PEAK FLUX = 2.6776E-04
LEVS = 0.5000E-04 * (-10.0, -9.0, -8.0,
-7.0, -6.0, -5.0, -4.0, -3.0, -2.0,
-1.0, 1.0, 2.0, 3.0, 4.0, 5.0,
6.0, 7.0, 8.0, 9.0, 10.0)

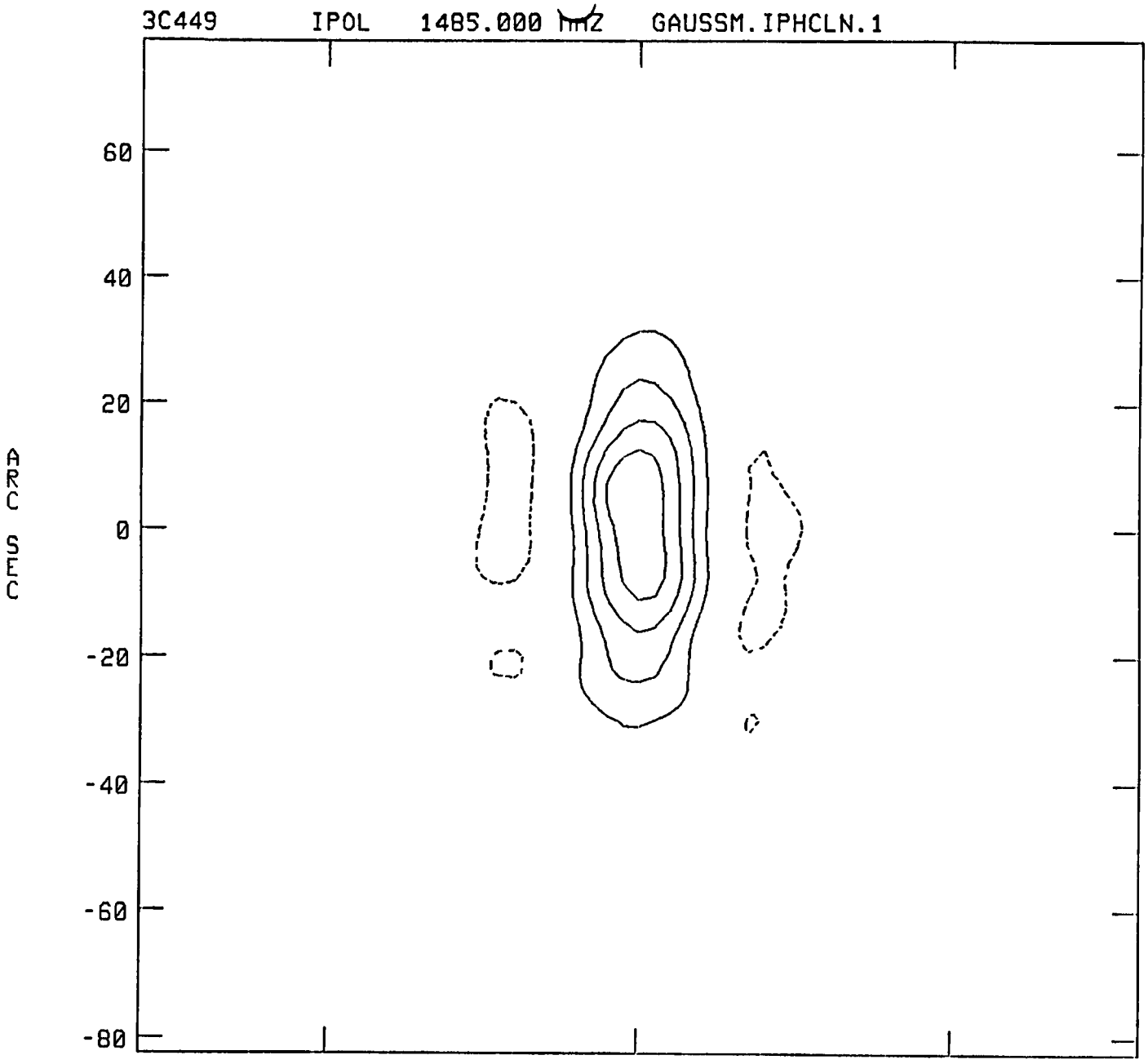

Phcln errors

CENTER AT RA 22 29 07.629 DEC 39 06 03.50
PEAK FLUX = 2.4293E-04
LEVS = 0.5000E-04 * (-10.0, -9.0, -8.0,
-7.0, -6.0, -5.0, -4.0, -3.0, -2.0,
-1.0, 1.0, 2.0, 3.0, 4.0, 5.0,
6.0, 7.0, 8.0, 9.0, 10.0)

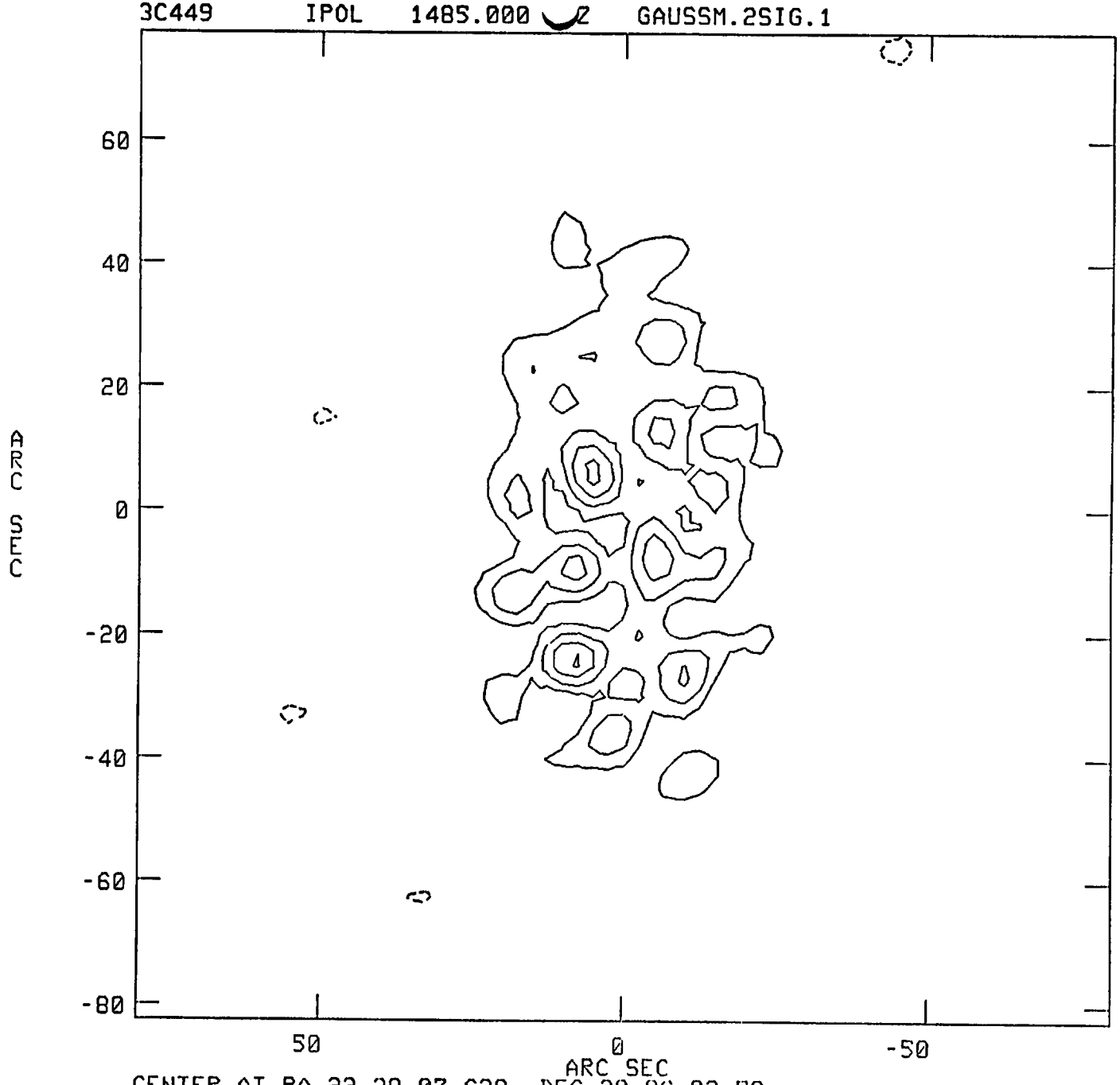

CENTER AT RA 22 29 07.629 DEC 39 06 03.50
PEAK FLUX = 2.1914E-04
LEVS = 0.5000E-04 * (-10.0, -9.0, -8.0,
-7.0, -6.0, -5.0, -4.0, -3.0, -2.0,
-1.0, 1.0, 2.0, 3.0, 4.0, 5.0,
6.0, 7.0, 8.0, 9.0, 10.0)

Fig 2

2σ H_1 emn)

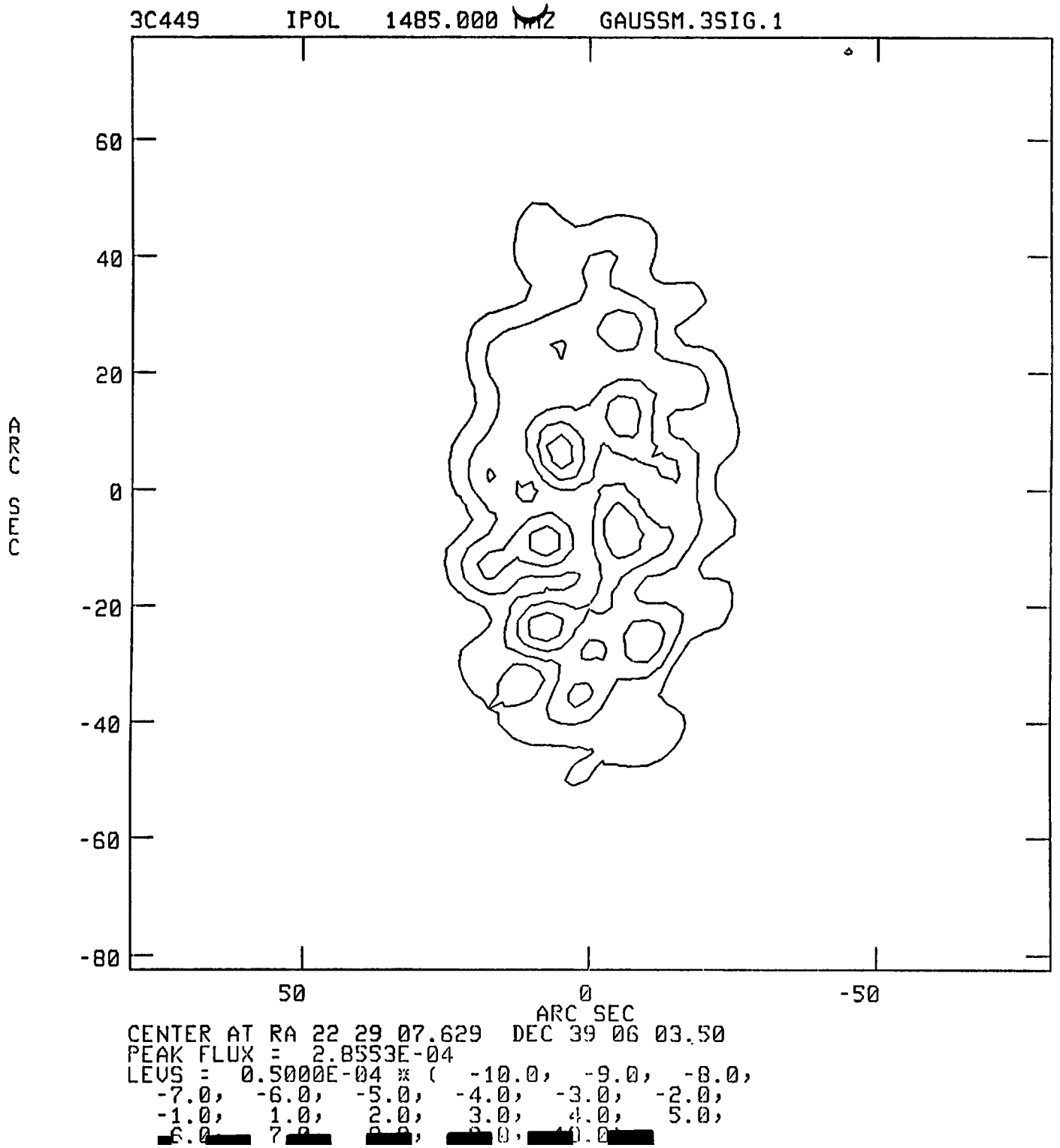
3C449 IPOL 1485.000 MHZ GAUSSM.3SIG.1
60
40
20
0
-20
-40
-60
-80
ARC SEC
50
0
-50
ARC SEC
CENTER AT RA 22 29 07.629 DEC 39 06 03.50
PEAK FLUX = 2.8553E-04
LEVS = 0.5000E-04 * (-10.0, -9.0, -8.0,
-7.0, -6.0, -5.0, -4.0, -3.0, -2.0,
-1.0, 1.0, 2.0, 3.0, 4.0, 5.0,

3σ H_1 emm

Fig 3 Gibbs Oscillations

True peak = 5×10^{-4}

$b_{upper} = 0.55$

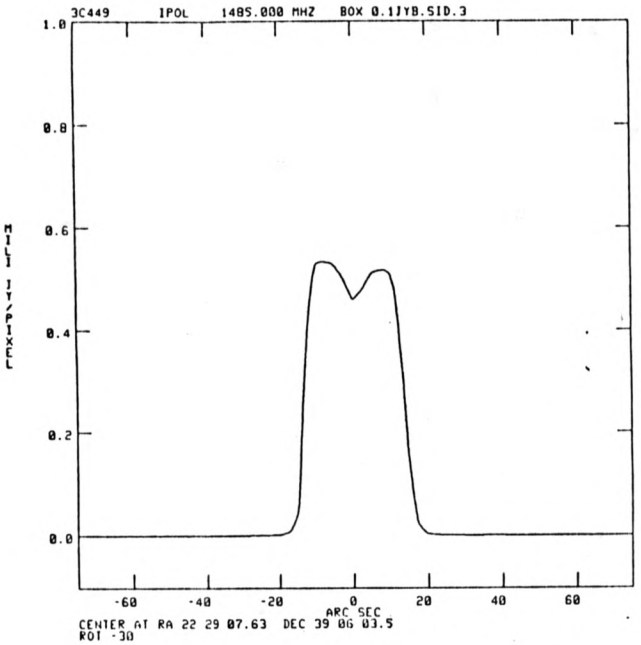

$b_{upper} = 0.6$

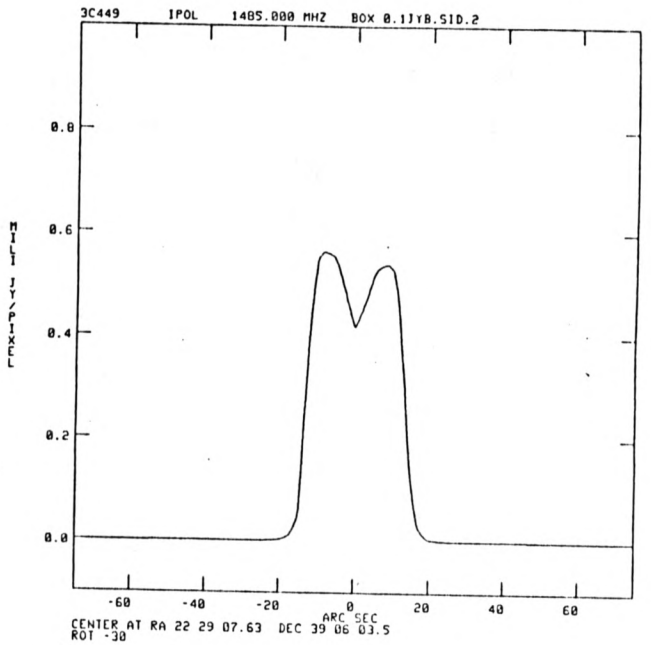

$b_{upper} = 0.505$

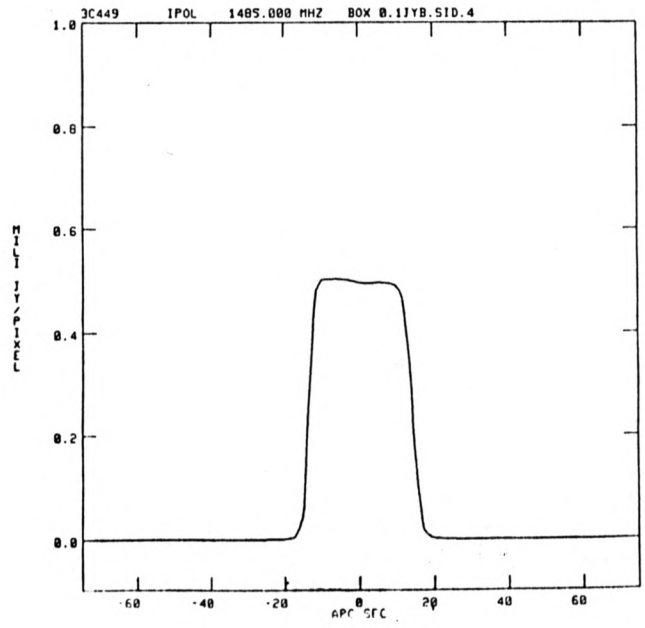

$b_{upper} = \infty$

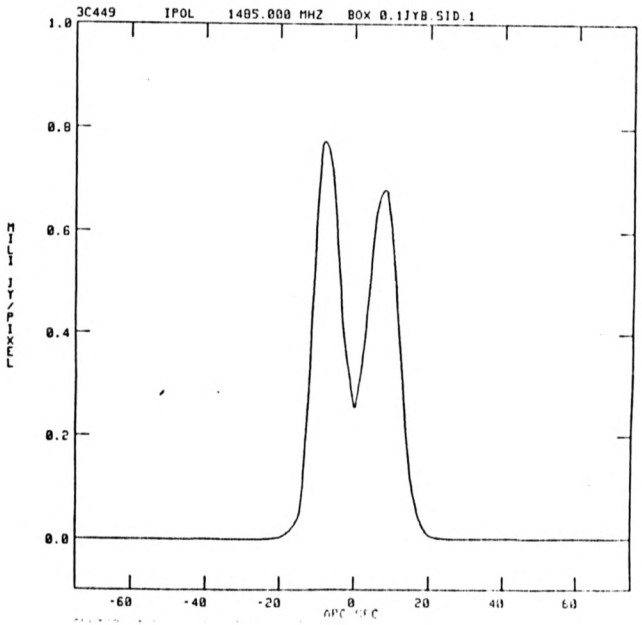

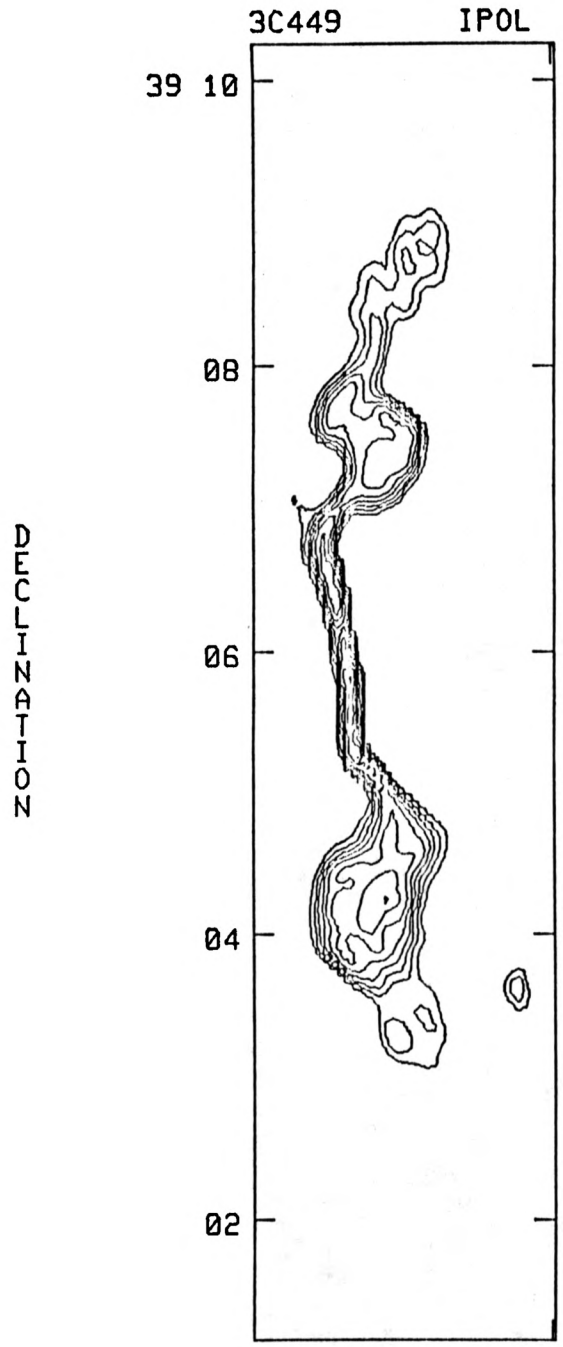

Fig 4(a)
C-array MERLIN image

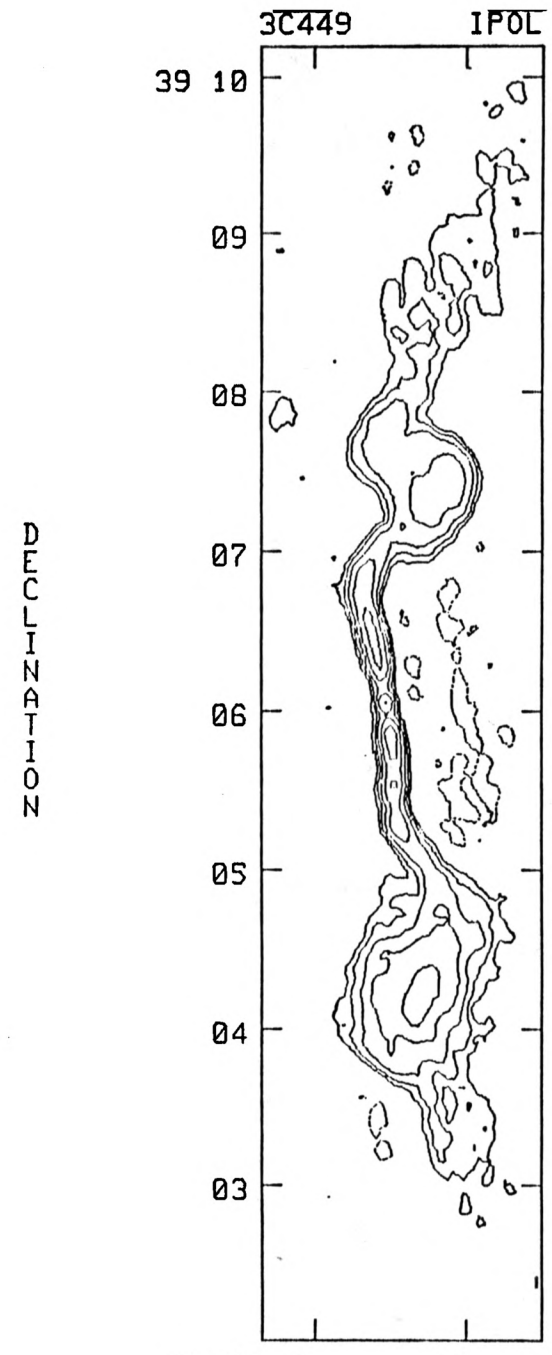

Fig 4(b)

B+C array CLEAN image

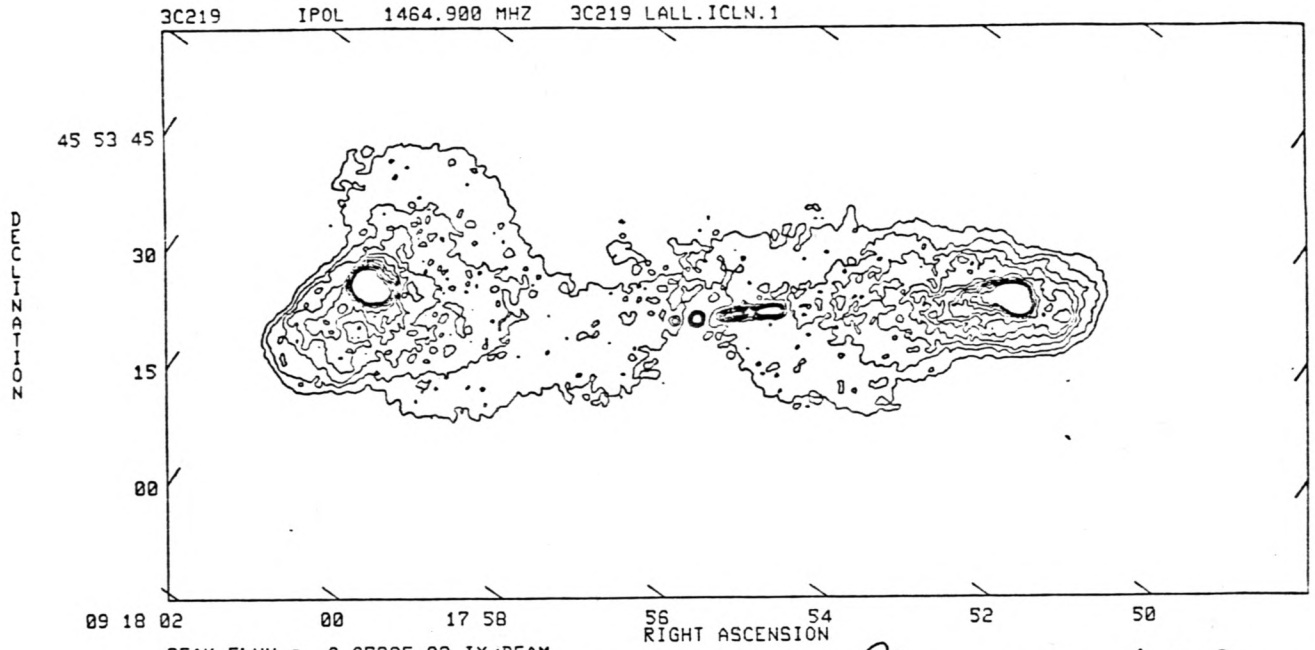

PEAK FLUX = 6.6508E-02 JY/BEAM
LEVS = 0.1330E-02 * (-10.0, -9.0, -8.0,
-7.0, -6.0, -5.0, -4.0, -3.0, -2.0,
-1.0, 1.0, 2.0, 3.0, 4.0, 5.0,
6.0, 7.0, 8.0, 9.0, 10.0)

Clean map A, B, D arrays

Fig 5

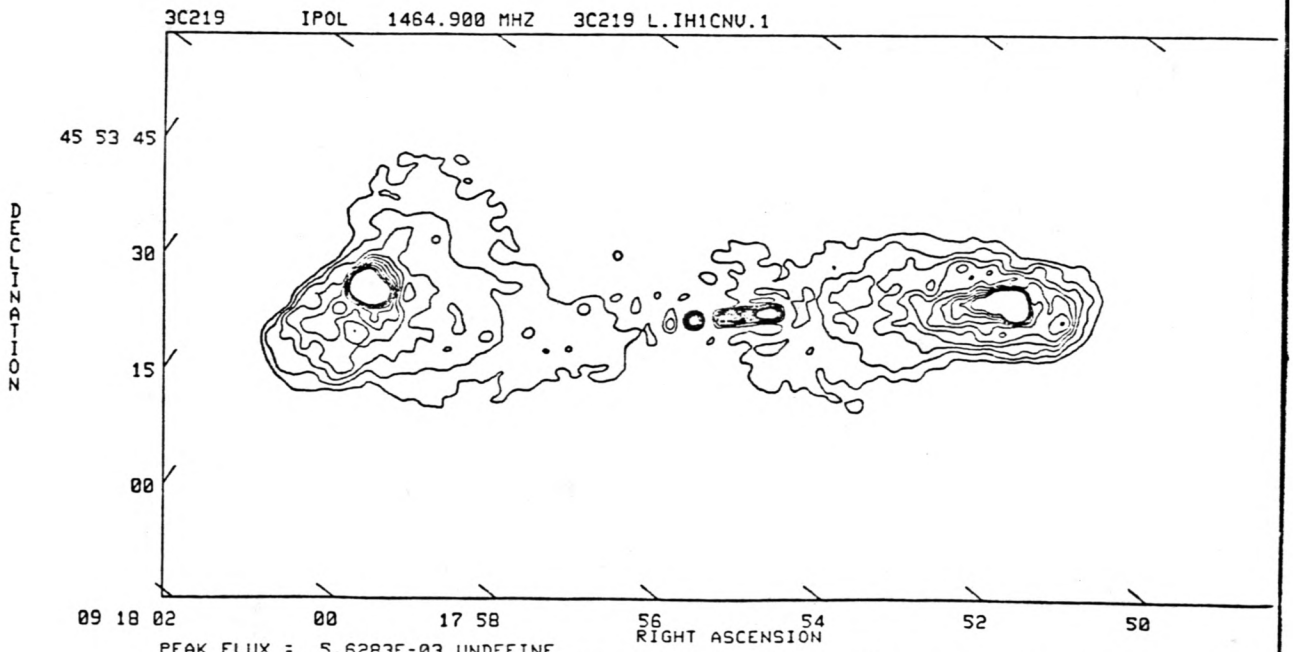

PEAK FLUX = 5.6283E-03 UNDEFINE
LEVS = 0.1126E-03 * (-10.0, -9.0, -8.0,
-7.0, -6.0, -5.0, -4.0, -3.0, -2.0,
-1.0, 1.0, 2.0, 3.0, 4.0, 5.0,
6.0, 7.0, 8.0, 9.0, 10.0)

H_1 map B, D arrays.

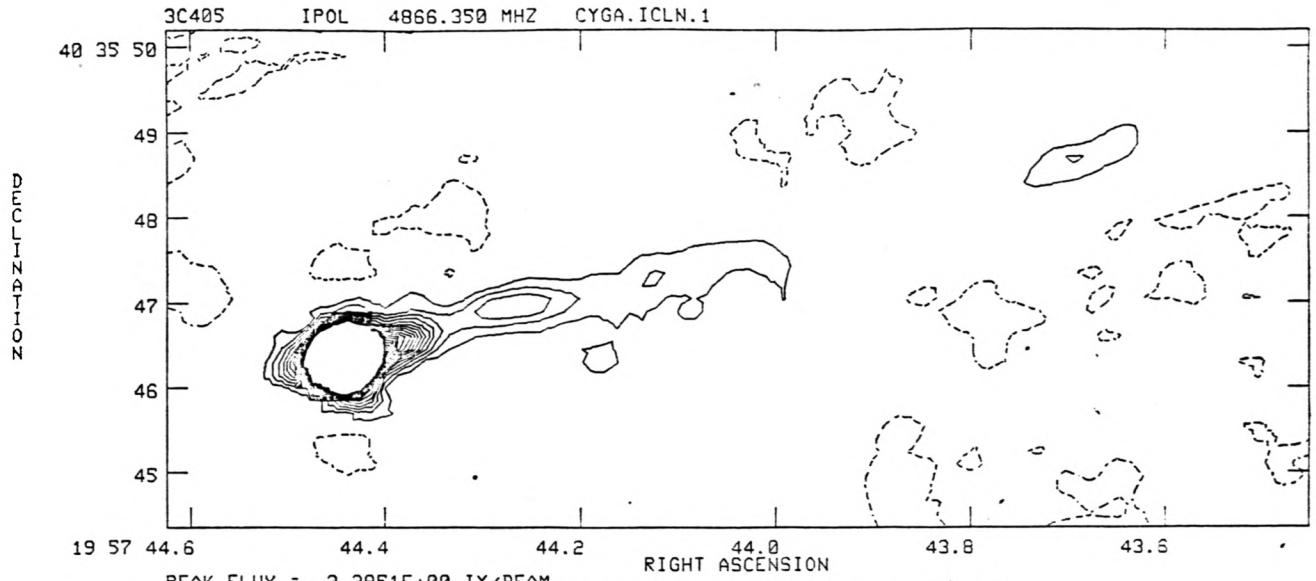

CLEAN

Fig 6 (a) Core + Jet

VM H_1

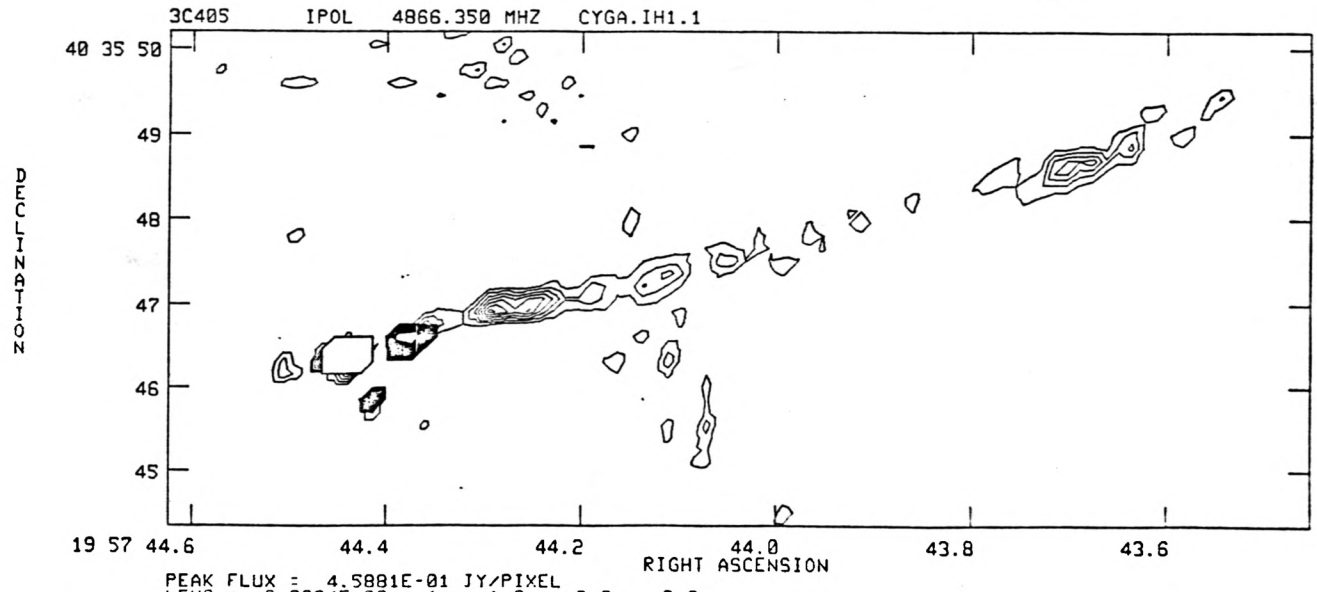

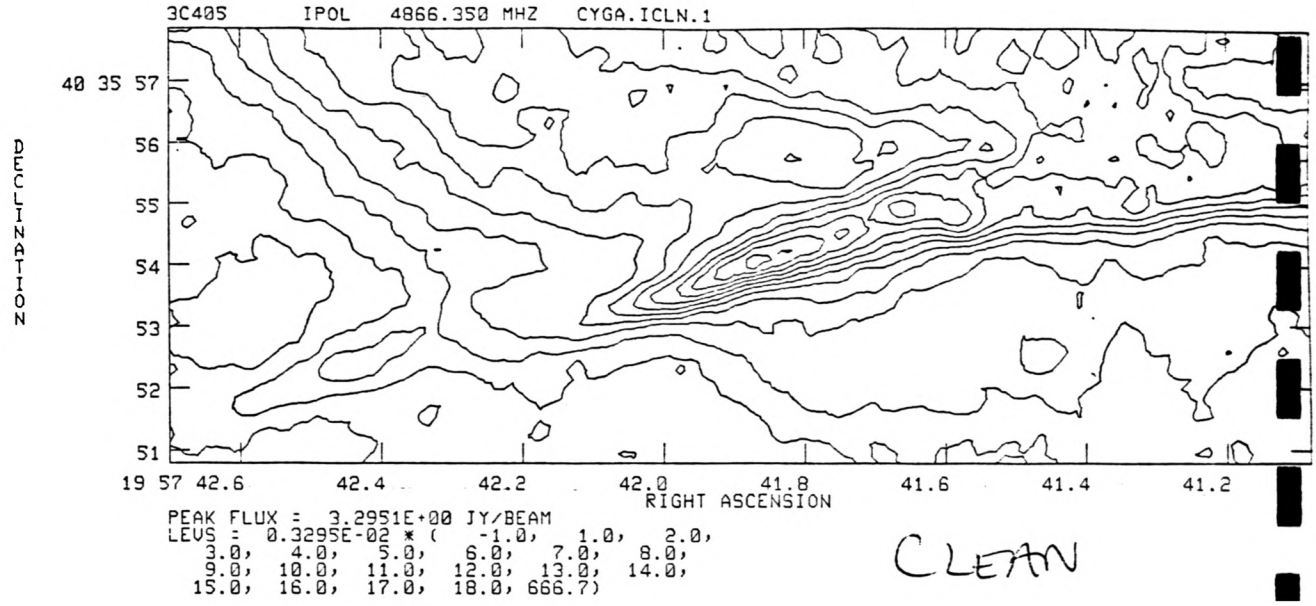

Fig 6 (b) jet entering lobe

VM H_1

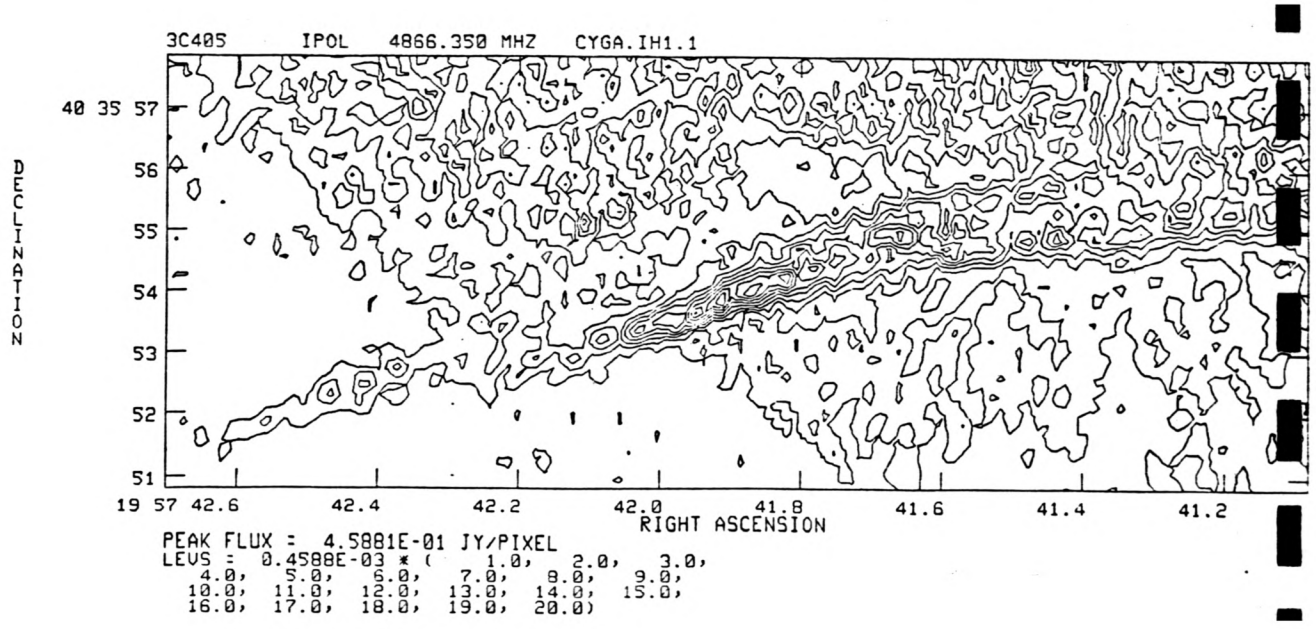

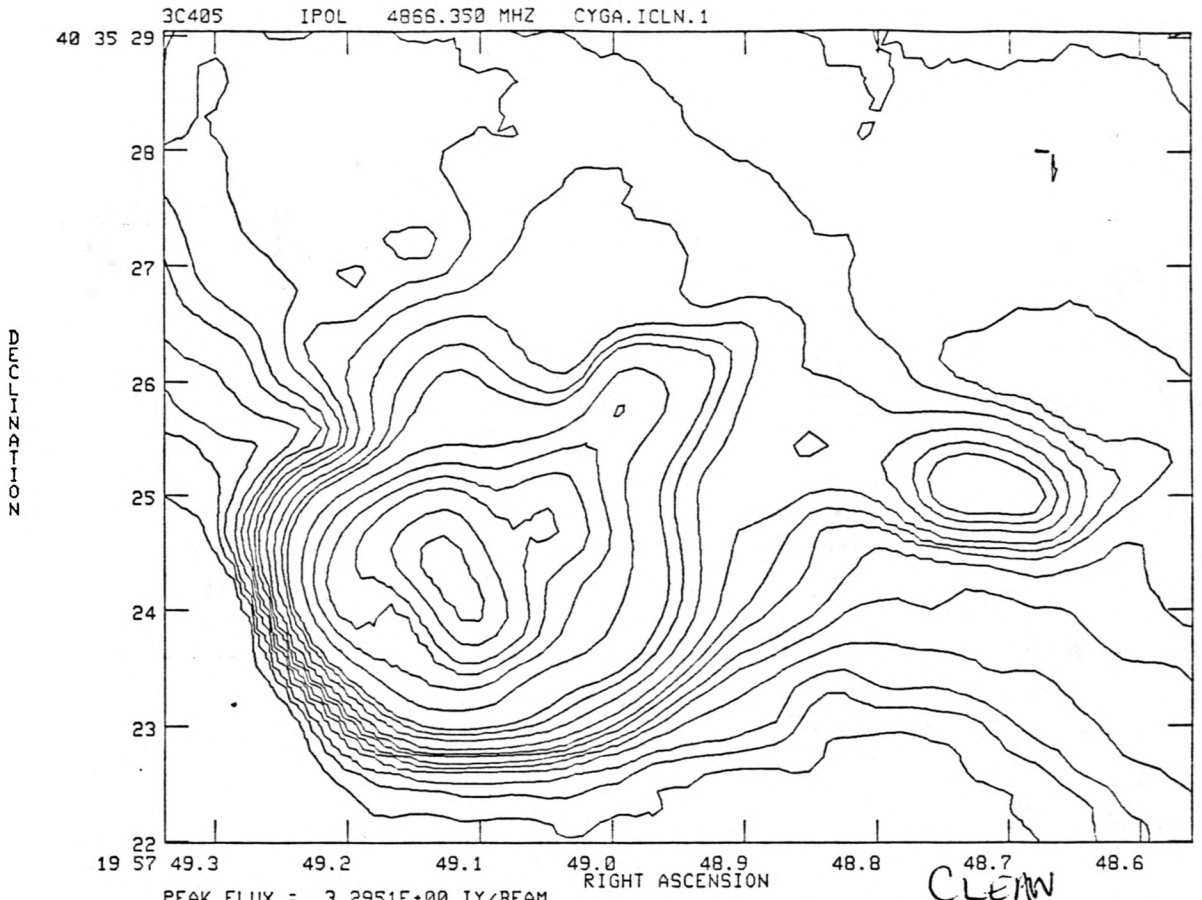

PEAK FLUX = 3.2951E+00 JY/BEAM
LEVS = 0.3295E-02 * (-1.0, 1.0, 2.0,
3.0, 5.0, 7.5, 10.0, 15.0, 20.0,
30.0, 50.0, 75.0, 100.0, 200.0, 300.0,
400.0, 500.0, 700.0, 900.0)

CLEAN

Fig. 6 (c) Sp 162e

VM H1

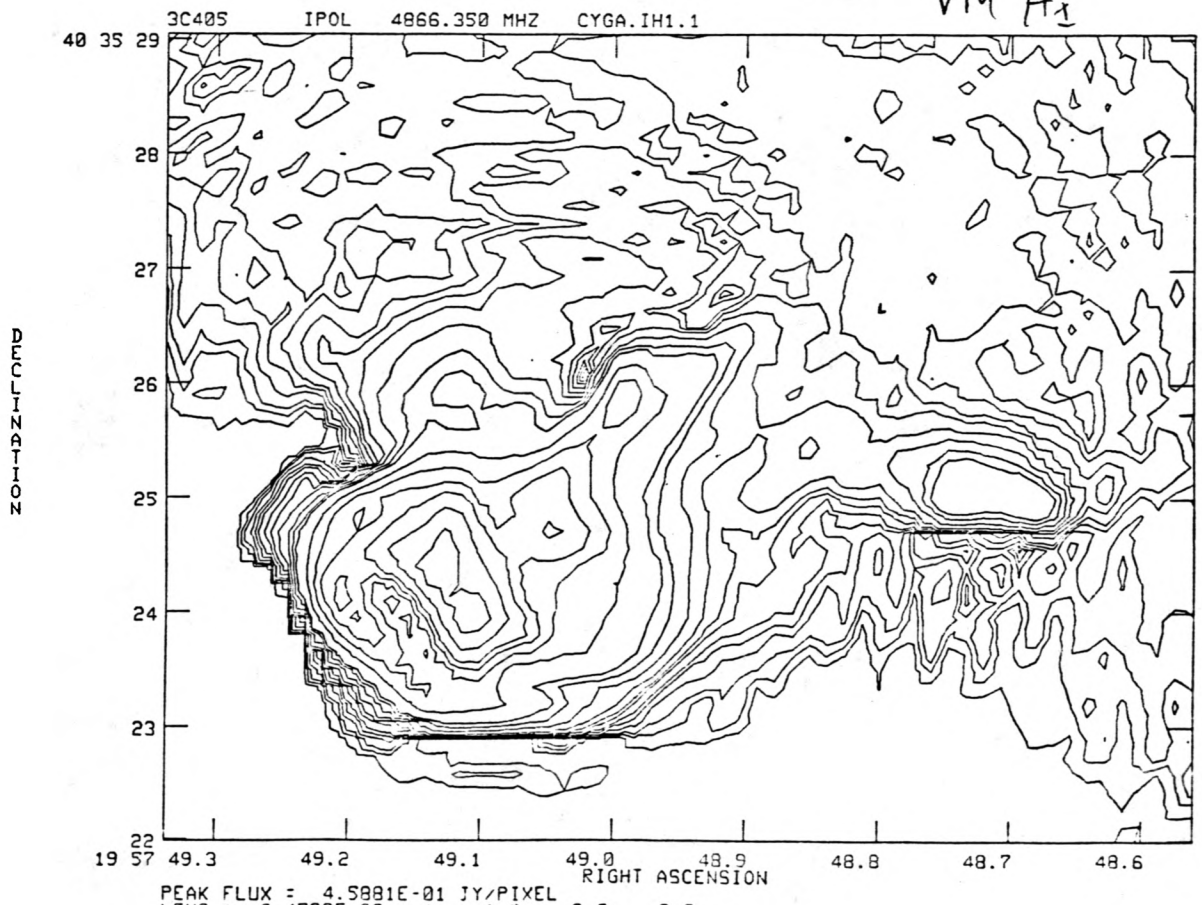

PEAK FLUX = 4.5881E-01 JY/PIXEL
LEVS = 0.4588E-03 * (1.0, 2.0, 3.0,
5.0, 7.5, 10.0, 15.0, 20.0, 30.0,
50.0, 75.0, 100.0, 200.0, 300.0, 400.0,
500.0, 700.0, 900.0)

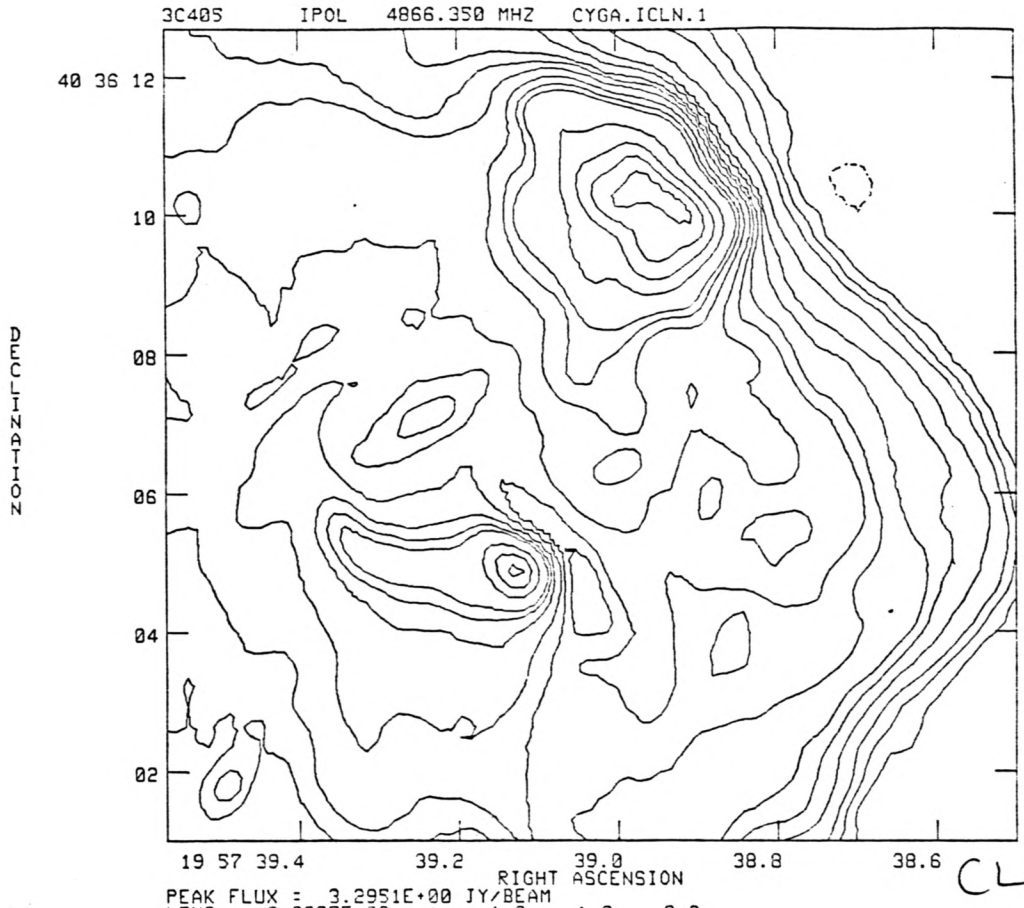

CLEAN

PEAK FLUX = 3.2951E+00 JY/BEAM
LEVS = 0.3295E-02 * (-1.0, 1.0, 2.0,
3.0, 5.0, 7.5, 10.0, 15.0, 20.0,
30.0, 50.0, 75.0, 100.0, 200.0, 300.0,
400.0, 500.0, 700.0, 900.0)

Nf lobe

Fig 6(d)

VM

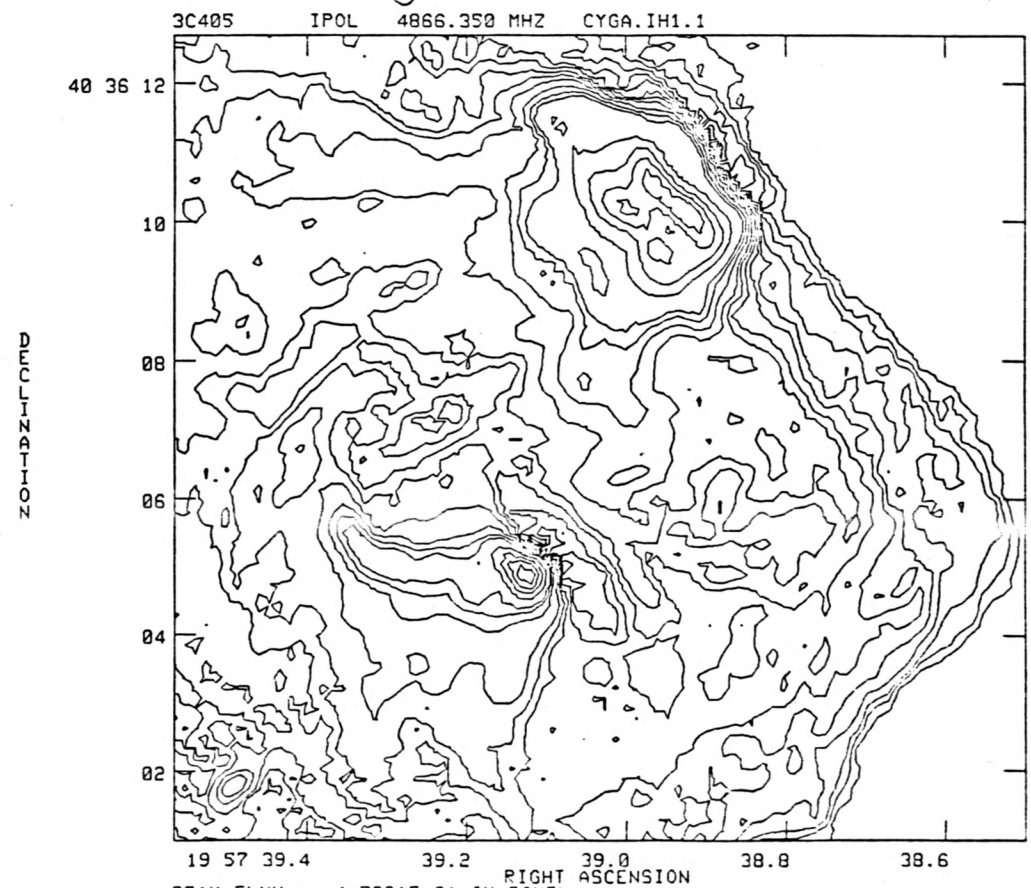

PEAK FLUX = 4.5881E-01 JY/PIXEL
LEVS = 0.4588E-03 * (1.0, 2.0, 3.0,
5.0, 7.5, 10.0, 15.0, 20.0, 30.0,
50.0, 75.0, 100.0, 200.0, 300.0, 400.0,
500.0, 700.0, 900.0)